



저작자표시-비영리-변경금지 2.0 대한민국

이용자는 아래의 조건을 따르는 경우에 한하여 자유롭게

- 이 저작물을 복제, 배포, 전송, 전시, 공연 및 방송할 수 있습니다.

다음과 같은 조건을 따라야 합니다:



저작자표시. 귀하는 원저작자를 표시하여야 합니다.



비영리. 귀하는 이 저작물을 영리 목적으로 이용할 수 없습니다.



변경금지. 귀하는 이 저작물을 개작, 변형 또는 가공할 수 없습니다.

- 귀하는, 이 저작물의 재이용이나 배포의 경우, 이 저작물에 적용된 이용허락조건을 명확하게 나타내어야 합니다.
- 저작권자로부터 별도의 허가를 받으면 이러한 조건들은 적용되지 않습니다.

저작권법에 따른 이용자의 권리는 위의 내용에 의하여 영향을 받지 않습니다.

이것은 [이용허락규약\(Legal Code\)](#)을 이해하기 쉽게 요약한 것입니다.

[Disclaimer](#)

Structural and functional brain alterations of post-chemotherapy cognitive impairment in gastric cancer

Jaeun Ahn

Department of Medicine

The Graduate School, Yonsei University

Structural and functional brain alterations of post-chemotherapy cognitive impairment in gastric cancer

Directed by Professor Young-Chul Jung

The Doctoral Dissertation
submitted to the Department of Medicine
the Graduate School of Yonsei University
in partial fulfillment of the requirements for the degree
of Doctor of Philosophy

Jaeun Ahn

December 2020

This certifies that the Doctoral
Dissertation of Jaeun Ahn is approved.

Thesis Supervisor: Young-Chul Jung

Thesis Committee Member#1: Kyung Ran Kim

Thesis Committee Member#2: Hyo Song Kim

Thesis Committee Member#3: Hae-Jeong Park

Thesis Committee Member#4: Soo-Hee Choi

The Graduate School
Yonsei University

December 2020

ACKNOWLEDGEMENTS

I would like to express my sincere gratitude to my thesis advisor Professor Young-Chul Jung for his patience, motivation, inspiration, and immense knowledge. He has been a true mentor and role model, and I could not wish for a better supervisor for my Ph.D. study. This dissertation would not have been possible without his keen guidance and unwavering support.

I am also indebted and grateful to my committee chair, Professor Kyung ran Kim, who provided support and invaluable advices for me to research.

I would like to thank my thesis committee members Professor Hyo song Kim, Hae-Jeong Park, and Soo-Hee Choi for their valuable suggestions and comments that enriched this study.

My sincere gratitude also goes to my mentors, Professor Dong-Ho Song and Keun-Ah Cheon, whose wholehearted guidance and motivation made this day possible. Furthermore, I would like to deeply thank all the professors and colleagues in the Department of Psychiatry at Yonsei College of Medicine. In particular, I am deeply grateful to Deokjong Lee, Junghan Lee and Junghee Ha who helped me in every aspect.

Last but not least, my special thank goes to my family: my parents, sisters, brother, and parents-in-law who always supported and guided me to dream and challenge myself, and also to my beloved daughter Claire and son John, whose mere presence gives me unbridled joy. In particular, I am grateful to my beloved husband Kwon who supported me through every step of the way. This thesis would not have been possible without you.

<TABLE OF CONTENTS>

ABSTRACT	1
I. INTRODUCTION	3
II. MATERIALS AND METHODS	7
1. Participants	7
2. Self-report questionnaires and neurocognitive assessment	8
3. Image acquisition	8
4. Voxel based morphometry analysis	9
5. Diffusion tensor imaging analysis	10
6. Resting state functional connectivity analysis	10
A. Region of interest (ROI) – based functional connectivity analysis	10
B. Graph theory – based network analysis: Minimum spanning tree analysis	12
7. Statistical analysis	14
III. RESULTS	14
1. Demographic characteristics	14
2. Neurocognitive results	20
3. Neuroimaging analysis	20
A. Voxel based morphometry analysis	20
B. Diffusion tensor imaging analysis	20
C. Resting state functional connectivity analysis	22
(1) Region of interest (ROI) – based functional connectivity analysis	22
(2) Graph-based network analysis: Minimum spanning tree	

analysis	24
IV. DISCUSSION	25
V. CONCLUSION	29
REFERENCES	30
ABSTRACT (IN KOREAN)	40

LIST OF FIGURES

Figure 1. Flowchart of the study	17
Figure 2. Decreased mean FA and increased mean MD among CTx+ group at 3 months follow up as compared to CTx+ group at baseline in left hippocampus.	21
Figure 3. When seeding from the left hippocampus, functional connectivity analysis showed significant group-by- time interaction in the anterior thalamus (red).	24

LIST OF TABLES

Table 1. Clinical characteristics of gastric cancer patients	16
Table 2. Demographic and clinical characteristics of gastric cancer patients and controls at baseline	18
Table 3. Neurocognitive assessment before and after chemotherapy	19
Table 4. Brain regions showing significant group by time interaction in the hippocampus-based functional connectivity analysis	23
Table 5. Brain regions showing significant group by time interaction in the 6 hippocampal subfields-based functional connectivity analysis	23

ABSTRACT

**Structural and functional brain alterations of post-chemotherapy
cognitive impairment in gastric cancer**

Jaeun Ahn

*Department of Medicine
The Graduate School, Yonsei University*

(Directed by Professor Young-Chul Jung)

Despite clinical significance of chemobrain, no longitudinal study has been made on change in cognitive function related to chemotherapy in gastric cancer. The aim of this study is to define structural and functional changes in brains of gastric cancer patients caused by chemotherapy-induced cognitive impairment after adjuvant chemotherapy. Thirteen gastric cancer patients with adjuvant chemotherapy (CTx+ group), nine gastric cancer patients without adjuvant chemotherapy (CTx- group), and ten healthy controls (HC) were enrolled for this study. We performed self-report questionnaires, neurocognitive tests, voxel-based morphometry (VBM), resting-state functional magnetic resonance imaging (rsfMRI) and diffusion tensor imaging (DTI) analysis twice at before and 3 months after chemotherapy. Compared to CTx- group, CTx+ group exhibited statistically significant decrease in attention and executive function over time, and also exhibited dysfunction in delayed recognition performance. DTI analysis had interesting results that

showed reduced fractional anisotropy (FA) and increased mean diffusivity (MD) in left hippocampus. In addition, results in resting state functional connectivity analysis show significant group-by-time interaction in left hippocampus-anterior thalamus. However, results from VBM analysis confirms that chemotherapy does not cause structural changes in brain. To the best of our knowledge, this is the first longitudinal neuroimaging study on the effect of chemotherapy in gastric cancer patients. Based on the results of this study, we suggest that neuropathological processes and clinical presentation of chemobrain is ultimately similar disease as age-related neurodegenerative disorder. Results of this study help in viewing underlying basis of chemobrain at a new angle and puts emphasis in importance of continuous assessment and intervention.

Key words: gastric cancer, post-chemotherapy cognitive impairment, neuroimaging, voxel-based morphometry, diffusion tensor imaging, resting state functional connectivity

Structural and functional brain alterations of post-chemotherapy cognitive impairment in gastric cancer

Jaeun Ahn

*Department of Medicine
The Graduate School, Yonsei University*

(Directed by Professor Young-Chul Jung)

I. INTRODUCTION

Chemotherapy-induced cognitive impairment, also referred to as chemobrain, is one of the most frequently reported side effects of chemotherapy and is an important dysfunction that is directly related to impaired social and occupational function and decreased quality of life ¹. After chemotherapy, 18%-78% of cancer patient experience cognitive impairment such as memory loss, apraxia, attention deficit, etc ^{2,3}. These symptoms may disappear in the short-term, but as many as 35% of chemotherapy patients suffer from continued symptoms even after months or years after complete recovery of cancer ³⁻⁵. In addition, considering that chemotherapy-induced cognitive impairment can increase the risk of dementia and stroke ^{6,7}, early detection of chemobrain has clinical significance.

As clinical significance of Chemobrain phenomenon is highlighted, related research is increasing, but nevertheless, because well-designed prospective studies are limited ⁸, precise structural and functional changes in the brain that underlie this dysfunction is also still uncertain. Although limited in numbers,

studies using structural neuroimaging technique and functional neuroimaging technique have helped us in understanding neural changes related to chemobrain in detail. Results of previous studies have revealed that objective, neuroimaging tests detect clear neural changes associated with chemobrain. And it seems chemotherapy has neurotoxic effect on frontal, temporal and parietal regions similar in age-related neurodegenerative disorders⁸. Beyond this, little is known with certainty. Majority of structural imaging studies using techniques such as voxel-based morphometry and diffusion-tensor imaging suggest that chemotherapy causes white and gray matter volume decrements and altered white matter microstructure⁹⁻¹². However, there is some disagreement concerning the duration of chemotherapy-induced structural changes⁸. Looking into functional imaging researches, we can find limited task-based fMRI researches; However, despite resting state fMRI being a powerful tool in studying functional brain network, no longitudinal evaluation of resting state fMRI on decline of cognitive function after chemotherapy has been carried out up to now⁸. Therefore, past studies has reported abnormality in domains included in DMN, which are most representative to resting state, particularly precuneus, medial frontal gyrus through meta-analysis using task-based fMRI as a basis to estimate resting state fMRI¹³. These results suggest disruption of modulation of DMN in chemobrain patients when performing various executive or memory tasks. And the results of fMRI studies so far have reported hypoactivation or hyperactivation in many different areas of brain, but the results thus far have only reported inconsistent changes in functional connectivity⁶. Considering ambiguity of results from past studies, it is of great clinical significance to study structural and functional neural change in brains of patients suffering from cognitive impairment symptom chemotherapy's neurotoxicity.

Although the neuropathological mechanisms underlying chemobrain is yet to be understood clearly, there have been evidences suggesting that hippocampus

may be an important area that is vulnerable to chemotherapy-induced neurotoxicity in recent studies ¹⁴. In various previous rodent researches, evidences proving that chemobrain is related to impaired neurogenesis of hippocampus ^{15,16}, neuroinflammation^{17,18}, oxidative stress, mitochondrial dysfunction^{19,20}, and structural damage to neurons have been cumulating. Several recent neuroimaging studies have reported reduced total volume and inward deformities in hippocampal subfields in breast cancer patients ^{21,22}. Hippocampus is also a key area in cognitive function such as memory formation, learning²³, spatial processing²⁴, memory recognition, prospective memory processing²⁵, etc.. Furthermore, hippocampus was once understood as a single structure, but recently it has been emphasized that hippocampus is not a homogenous structure, but a domain consisting of several subfields with different histological characteristics and function²⁶. However, there is a need for research on the structural and functional changes of hippocampus in chemobrain, considering that they remain unknown.

Most of studies on chemobrain until now not only have been carried out on breast cancer patients due to reasons such as high survival rates of breast cancer, and potentially higher likelihood of female patients to report perceived changes in cognitive abilities ^{27,28}. However, based on the fact that the chemobrain phenomenon is not limited to breast cancer ²⁹, we planned to study gastric cancer patients. Globally gastric cancer is major cause of morbidity and mortality with increasing number of total incident cases ³⁰. Especially in South Korea, gastric cancer is the most prevalent cancer in male of age 35 to 65 ²⁷ with the 5-year survival rate of around 71.5%, it is important to consider life after cancer of these patients ²⁸. In addition, because incidence age of gastric cancer is getting lower ³¹, cognitive function after chemotherapy is becoming more important in order for patients to maintain social and occupational function. Furthermore, since it is still unclear whether chemobrain phenomenon is a side effect of chemotherapy or reflect a more general comorbidity of cancer ^{32,33}, gastric

cancer is well suited to study chemobrain phenomenon because while brain metastases from breast cancer are second in line after lung cancer (13-19%)³⁴, brain metastases in gastric cancer is exceedingly rare and diagnosed in <1% of affected patients³⁵. Despite such phenomenon, no longitudinal study has been made until now on change in cognitive function related to chemotherapy in gastric cancer. From this point of view, research on gastric cancer patients help us understand which domain of cognitive function is affected and which neural changes are caused by chemotherapy, and therefore has great clinical significance for gastric cancer patients.

In this study, we aimed to study comprehensive underlying mechanism of chemobrain through multimodal neuroimaging analysis including VBM, rsfMRI and DTI. First of all, we checked alterations in attention and concentration, memory, executive function of both patients with scheduled adjuvant chemotherapy (CTx+ group) and patients who do not need adjuvant chemotherapy (CTx- group) at the time of baseline and follow up through neurocognitive assessment. Afterwards, we implemented neuroimaging analysis focusing on areas where the difference between baseline and follow-up was confirmed through the neurocognitive assessment. As for neuroimaging analysis, we attempted to identify whether there is Chemobrain underlying structural brain change through gray matter changes in VBM analysis. Secondly, we applied seed based resting state functional connectivity analysis to investigate neural network changes in chemobrain. Lastly, we attempted to identify how functional change is related to change in white matter microstructural integrity through DTI analysis. Until now, no other longitudinal DTI studies of white matter chemotherapy-induced changes have been performed for gastric cancer patient. Anticancer agents are known to cause extensive damage in myelin which is hallmark of WM tracts in experimental research (Han et al., 2008b).

As mentioned above, this study aims to achieve in depth understanding of cognitive impairments underlying neural change of gastric cancer patients after

chemotherapy through longitudinal study using various multimodal neuroimaging techniques. To the best of our knowledge, this longitudinal research is the first research aiming to identify chemobrain underlying structural and functional changes in gastric cancer patients with focus on hippocampus using neuroimaging techniques.

II. MATERIALS AND METHODS

1. Participants

This prospective study was approved by the Institutional Review Board of Severance Hospital, and informed written consent was obtained from all subjects before each procedure. Male gastric cancer patients between age 40 and 60 who underwent total gastrectomy or partial gastrectomy (distal gastrectomy, subtotal gastrectomy) were enrolled in this study. Candidates were divided into two groups: patients with scheduled adjuvant chemotherapy (CTx+ group) and patients who do not need adjuvant chemotherapy (CTx- group). In addition, Age- and sex-matched healthy controls (HC group) without cognitive impairment or active neurological disorders were also recruited as a control group. Participants who had (1) history of other malignancy, (2) history of metastatic malignancy, (3) history of any neurologic condition that could impair cognitive function (neurodegenerative disease, stroke, brain injury, etc.), (4) history of any neurologic condition that could impair cognitive function (dementia, stroke, brain injury, etc.), (5) history of alcohol, nicotine, caffeine, or other drug dependence or addiction and (6) psychiatric Axis I disorder were excluded in this study.

Initial baseline assessment was performed on CTx+ group (n = 19, age 49.2 ± 5.5) and CTx- group (n = 14 age 49.2 ± 6.8) and HC group (n=10, age 51.5 ± 7.0). Baseline assessment was performed by carry out self-report questionnaires assessment, neurocognitive assessment, and magnetic resonance

imaging (MRI) scan all on the same day, after gastric cancer surgery and before adjuvant chemotherapy. In CTx+ group, follow-up assessment was performed around 3 months past baseline assessment, after the subject underwent adjuvant chemotherapy. CTx- group was also assessed on matched intervals.

2. Self-report questionnaires and neurocognitive assessment

Self-report questionnaires contained the Cognitive Failure Questionnaire (CFQ)³⁶ to assess subjective cognitive decline; the Beck Depression Inventory (BDI)³⁷ to assess depressive symptoms; and the Beck Anxiety Inventory (BAI)³⁸ to assess anxiety symptoms. All subjects carried out Structured Clinical Interview, and assessment on major psychiatric illness was performed according to the Diagnostic and Statistical Manual of Mental Disorders, Fourth Edition³⁹. Four cognitive domains were assessed using a set of neurocognitive tests: (1) performance and verbal intelligence [Korean version of Wechsler Adult Intelligence Scale (K-WAIS) performance and verbal subtests]; (2) memory (Rey-Kim Memory Test); (3) attention (K-WAIS digit span and spatial span subtest); and (4) executive function (stroop Test). Scores for the neurocognitive tests were expressed as age corrected scaled scores (AgeSS), standardized scores (SS), or percentile ranks for raw scores.

3. Image acquisition

All subjects were imaged on a 3.0 T MRI scanner (Tim Trio, Siemens Healthcare, Erlangen, Germany) and images including T1-weighted imaging, diffusion tensor image and resting state fMRI were obtained. A 3D T1-weighted anatomical image was obtained using a spoiled gradient-echo sequence (sagittal acquisition with TR = 1900 msec; TE = 2.52 msec; FOV = 256 × 256 mm²; voxel size = 1 × 1 × 1 mm³; flip angle 9°; slice number = 176; and total acquisition time 4 min 26 sec) to serve as an anatomical underlay for the brain activity and to be used for grey matter volume analysis. diffusion tensor image

were acquired with the following echo planar acquisition parameters: diffusion-weighted gradients applied in 30 non-linear directions, number of average = 2, TR = 6200 ms, TE = 85 ms, flip angle = 90°, acquisition matrix = 128 × 128, FOV = 230 × 230 mm², slice thickness = 3 mm, and b value = 600 s/mm². Resting state functional images were acquired using gradient echo-planar pulse imaging (EPI). For each subject, 150 axial volume scans were obtained with the following parameters: TR = 3000 msec, TE = 30 msec, FOV = 192 × 192 mm², voxel size = 3×3×3 mm³, slice number = 50 (interleaved). All participants were instructed to rest and keep their eye closed without sleeping, moving, or thinking about anything during the scan (7min 30sec). Vacuum-molded cushions and soft pads were used to support the head and minimize head movement.

4. Voxel based morphometry analysis

All preprocessing steps were conducted in accordance with the standardized procedure⁴⁰. First, the structural images were aligned along the anterior–posterior commissure line and positioned so that the anterior commissure matched the origin. Afterward, the images were segmented into gray matter, white matter and cerebrospinal fluid probability maps by using a Bayesian image segmentation algorithm. Brain tissue probability maps for each subject were then used for intersubject alignment. In this study, we applied diffeomorphic anatomical registration by using an exponentiated Lie algebra algorithm (DARTEL)⁴⁰. The DARTEL has been suggested to enhance the accuracy of intersubject alignment, by modeling the shape of each brain by using a host of parameters. The DARTEL processing involves generating the flow fields that parameterize the deformations and creating the templates for all subjects. After the final study-specific template was created, gray matter images for each subject were warped to the study-specific template and then normalized into standard Montreal Neurological Institute space. The volumes were resampled to 1.5 × 1.5 × 1.5 mm³ voxel size. This spatial normalization step

included Jacobian modulation in order to preserve regional volume data. Finally, the DARTEL-warped, normalized and modulated gray matter images were smoothed by using 8-mm full-width at half maximum kernel.

5. Diffusion tensor imaging analysis

diffusion tensor image data were analyzed using diffusion MR toolbox ‘Explore DTI’⁴¹ and following steps were performed: (i) correction for subject motion and eddy current induced distortions⁴²; (ii) tensor estimation using the REKINDLE approach for outlier detection⁴³ with iteratively reweighted linear [least squares](#) estimation after identification and removal of data outliers⁴⁴; and (iii) automated atlas based analysis with the SRI24 Atlas (normal adult brain anatomy;⁴⁵ using affine and elastic registration based on ‘elastix’⁴⁶. All diffusion tensor image data were visually checked in terms of quality of tensor estimation and quality of registration. After these preprocessing steps, FA, AD, RD, and MD values were calculated in the bilateral superior parietal lobe, superior frontal gyrus and hippocampus that are provided by the SRI24 Atlas (Rohlfing et al., 2010).

6. Resting state functional connectivity analysis

A. Region of interest (ROI) – based functional connectivity analysis

Spatial preprocessing and statistical analyses of functional images were performed using SPM12 (Wellcome Trust Centre for Neuroimaging). To analyze functional connectivity of resting state functional MRI, motion artifacts were assessed in individual subjects by visually inspecting realignment parameter estimations to confirm there were no abrupt head motions and the maximum head motion in each axis was <3 mm. Functional images were realigned and registered to structural images for each subject. The anatomical volume was segmented into gray matter, white matter, and cerebrospinal fluid. The gray matter image was used for determining the parameters of

normalization onto the standard Montreal Neurological Institute (MNI) gray matter template provided with SPM12. The spatial parameters were then applied to the realigned functional volumes that were finally resampled to voxels of $2 \times 2 \times 2 \text{ mm}^3$ and smoothed with an 8 mm full-width at half-maximum kernel.

The assessment of cortical networks was performed using a ROI seed-based correlation approach. Connectivity analysis was conducted with the “conn” toolbox, implemented in the SPM12 (<http://www.fil.ion.ucl.ac.uk/spm/ext>). Seed areas were chosen using the automated anatomical labeling (aal) template (www.fil.ion.ucl.ac.uk/spm/ext/) (Tzourio-Mazoyer et al., 2002). According to result of the neurocognitive assessment of between-group differences over time, we designated the superior parietal lobe, which is associated with spatial span (Berryhill and Olson, 2008), bilateral hippocampus, which is associated with recognition (Fontán-Lozano et al., 2007; Zhou et al., 2010; Pospisil et al., 2015), and bilateral superior frontal gyri, which is associated with executive function(SFG) as the seed region in our study. Recently, there has been an accumulation of evidence that hippocampus is divided into several subfields, and each has a specific cognitive function. In particular, it is argued that neurodegenerative disorder patients show the sequential pattern of change in brain starting within entorhinal and transentorhinal areas and moving to cornu ammonis area 1 (CA1), subiculum and eventually other subfields. To study acute neurotoxic effect of chemotherapy, we conducted further analysis by classifying 6 subfields of hippocampus and setting them as seed region. ROI for subfields of bilateral hippocampus (consisting of cornu ammonis (CA), including CA1,CA2, and CA3 subfields; dentate gyrus (DG), including fascia dentata and the CA4 subfield; and subiculum (SB), including the prosubiculum, subiculum proper, presubiculum and parasubiculum) was obtained from the the maximum probability map(MPM) ⁴⁷ and was defined using the Anatomy toolbox v22c implemented on SPM12 (www.fil.ion.ucl.ac.uk/spm). The waveform of each brain voxel was temporally filtered by means of a bandpass

filter ($0.008 \text{ Hz} < f < 0.09 \text{ Hz}$) to adjust for low-frequency drift and high-frequency noise effects. A linear regression analysis was conducted to remove signals from the ventricular area and the white matter⁴⁸. Movement parameters were added as first-level covariate. The between-group, within-group longitudinal comparisons, and group-by-time interactions analyses were compared with an uncorrected p-value height threshold of 0.001 and $k=90$ as extent threshold for the whole brain. To estimate the strength of an FC, correlation coefficients were computed and converted to z-values using Fisher's r-to-z transformation.

B. Graph theory-based network analysis: Minimum spanning tree analysis

Image preprocessing was performed using the FMRIB's Software Library (FSL)⁴⁹ and the brain was automatically extracted from the T1-weighted scan⁵⁰. Time series were motion corrected with MCFLIRT^{51,52}. This removes subject's head movement and allows calculation of the mean relative displacement. Participants with a mean relative displacement larger than 0.2 mm were excluded⁵³. Six motion components were extracted, i.e. three voxel-wise displacement parameters and the temporal signal intensities obtained from white matter, cerebrospinal fluid, and global time courses⁵⁴. The functional scan was registered to the high-resolution anatomical image by using rigid registration. The anatomical scan was subsequently matched with the Montreal Neurological Institute (MNI) 152 T1-weighted 2 mm image in standard space with affine registration. Functional scans were slice-time corrected, spatial smoothed to reduce noise (5 mm full-width-half-maximum). The first 15 volumes were deleted to ensure stabilized magnetization. Average time series from the cerebral spinal fluid, the white matter and grey matter intensities were determined after

tissue segmentation Tool (FAST) ⁵⁵.

The standard FSL pipeline is not sufficient to remove motion artifacts from the data, therefore additional motion correction is necessary ^{53,54,56-58}. Out of two additional motion correction methods, i.e. independent component analysis-based strategy for Automatic Removal of Motion Artifacts (ICA-AROMA) ^{58,59} and spike regression ^{53,54}, we selected the most effective one in controlling motion effects in our dataset for final correction. Volumes that exceeded the threshold of 0.2 mm framewise displacement ⁶⁰ were removed and a regression analysis with 24 motion components was done. Motion components were: three voxel-wise displacement parameters and their white matter, cerebrospinal fluid, global time courses, the quadrates, temporal derivatives and quadrates of the derivatives of these six parameters ⁶¹. A band-pass filter (0.01–0.08 Hz) was applied ⁵⁴. If the remaining data was <300 s, the subject was excluded from further analysis ⁶².

We selected 90 regions from the AAL brain atlas (V4) that cover the cortical and subcortical regions ⁶³. To estimate 90 regional mean time series, voxel time series within each AAL region were averaged. A correlation network was constructed for every participant, based on those time series using Pearson's correlation. Only positive correlations were taken into account as a result of the minimum spanning tree analysis, thus avoiding the problematic interpretation of negative BOLD correlations ^{64,65}. Mean connectivity strength of the network was calculated per subject. Minimum spanning tree network backbones were extracted with Kruskal's algorithm ⁶⁶ (MATLAB, version R2016b). For each minimum spanning tree, the diameter, kappa, tree hierarchy and leaf fraction were calculated.

To localize possible alterations in network organization to anatomical regions, regional network characteristics were analyzed. Since global network characteristics were analyzed based on the minimum spanning tree, we also focused on minimum spanning tree characteristics for regional analysis ⁶⁵. The

minimum spanning tree outcomes leaf fraction, diameter, kappa and tree hierarchy were compared between groups and within-group longitudinal comparisons. Regional minimum spanning tree characteristics were also tested between groups and within-group longitudinal comparisons.

7. Statistical analysis

Baseline demographic characteristics including age, years of education and results from self-report questionnaires were compared between gastric cancer patients with one-way ANOVA. In analyzing results from neurocognitive assessment, we compared changes in performance status of neurocognitive test before and 3 months after adjuvant chemotherapy with a repeated measures ANOVA for a significance level of $P = 0.05$ between CTx+ group and CTx-group.

In case of DTI parameters (FA, AD, RD, and MD values) calculated from DTI analysis, between group, analysis on between group difference was evaluated through two sample t-test, and in case of within group analysis, within group differences were evaluated through paired t-tests with Bonferroni correction for multiple comparisons. All statistical analysis were conducted by using SPSS 25.0 (IBM, Armonk, NY, USA).

III. RESULTS

1. Demographic characteristics

At baseline, 19 gastric cancer patients who underwent total gastrectomy or subtotal gastrectomy and were candidates for adjuvant chemotherapy and 14 patients who underwent total gastrectomy or partial gastrectomy (distal gastrectomy, subtotal gastrectomy) but not adjuvant chemotherapy were

enrolled in this study. Of the 19 patients who received adjuvant chemotherapy after surgery, 6 were excluded as 2 patients expired during chemotherapy and 4 refused follow-up assessment after chemotherapy. 5 patients who were enrolled in CTx- group were excluded as well because they refused follow-up assessment. Age-matched 13 healthy men were recruited as control subjects. Among them, 2 healthy control participants were excluded since they showed cognitive impairment on the neurocognitive tests. And 1 healthy control participant excluded due to fail to perform multimodal neuroimaging studies. No participant was excluded due to excessive head movement during fMRI scanning. Therefore, the final sample size for the longitudinal analysis was total of 38, and all subjects had completed formal education. The breakdown of sample size is as follows: 13 for the CTx+ group, 9 for the CTx- group, and 10 for the control group (Fig 1).

CTx+ group consisted of 1 cancer stage I patient, 3 cancer stage II patients, 8 cancer stage III patients, and 1 cancer stage IV patient, and went through XELOX or TS-1 regimen chemotherapy. CTx- group consisted of 3 cancer stage I patients, and 6 cancer stage II patients. TS-1 regimen is a regimen with a one year schedule that repeats 4 weeks of chemotherapy followed by 2 weeks of break and begins 6 weeks after surgery. XELOX is an anti-cancer medication that follows schedule of 8 cycle treatments at 3 week interval. In case of CTx+ group, follow-ups were made at 94.5 ± 10.5 days after surgery on average, and in case of CTx-group, follow-ups were made at 92.6 ± 11.1 days after surgery on average. Implemented surgery type, protocol of adjuvant chemotherapy and cancer stages of patients are summarized in Table 1. At baseline, there was no significant difference between the two groups in terms of age, duration of education, CFQ score, BDI score and BAI score (Table 2).

Table 1. Clinical characteristics of gastric cancer patients

	CTx + (n=13)	CTx - (n=9)
Surgery type		
Total gastrectomy	4	0
Subtotal gastrectomy	8	2
Distal gastrectomy	1	7
Cancer stage		
I	1	3
II	3	6
III	8	0
IV	1	0
Protocol of adjuvant chemotherapy		
XELOX	7	N/A
TS-1	6	N/A

Notes: CTx+: Patients Treated with Chemotherapy; CTx-: Patients Not Treated with Chemotherapy; XELOX: oxaliplatin + Xeloda; TS-1 : Tagafur + Gemaracil

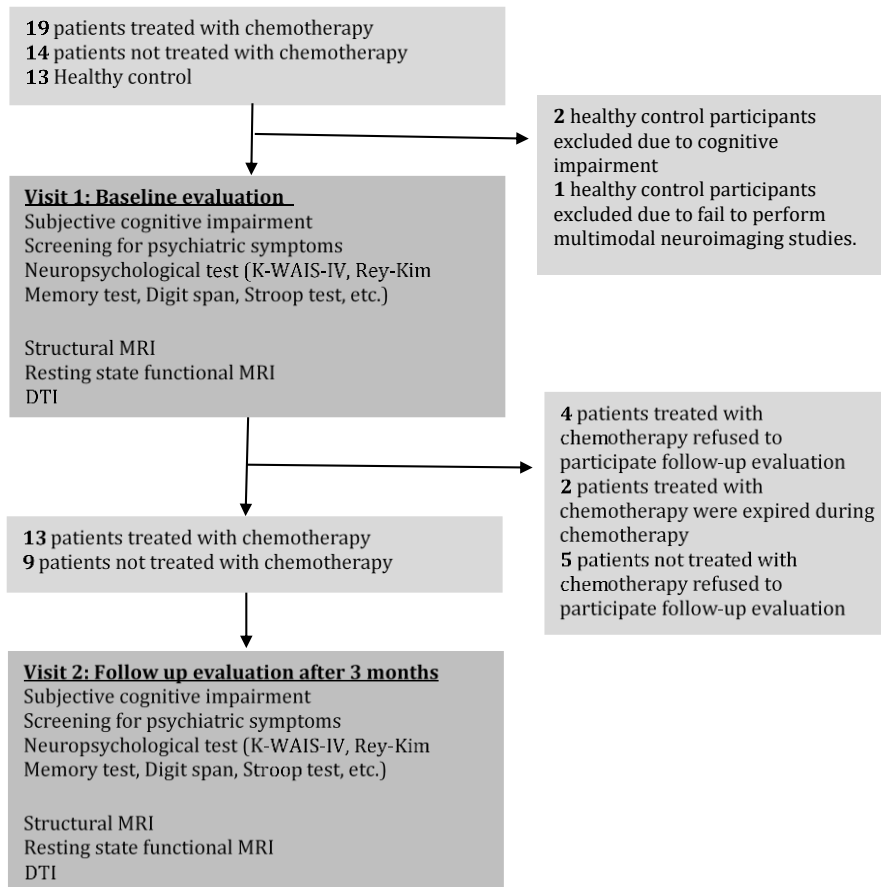


Figure 1. Flowchart of the study Note:DTI: Diffuse Tensor Image analysis; K-WAIS-IV: Korean **W**echsler Adult Intelligence Scale-IV; MRI: Magnetic resonance imaging

Table 2. Demographic and clinical characteristics of gastric cancer patients and controls at baseline

	CTx+ (n=13)	CTx- (n=9)	HC (n=10)	F	<i>p</i>
Age (years)	49.2±5.5	49.2±6.8	51.5±7.0	0.472	0.628
Years of education	13.1±3.2	13.3±2.0	12.7±1.6	0.189	0.828
BDI	9.8±7.4	8.2±6.8	10.7±6.9	0.366	0.696
BAI	6.0±6.6	6.9±5.4	6.2±5.9	0.075	0.928
CFQ	9.5±9.7	16.8±11.0	19.8±16.3	2.248	0.121

Notes: Means are presented followed by standard deviations

BDI: Beck Depression Inventory; BAI: Beck Anxiety Inventory; CFQ: Cognitive Failure Questionnaire; CTx+: Patients Treated with Chemotherapy; CTx-: Patients Not Treated with Chemotherapy; HC: Healthy Control

Table 3. Neurocognitive assessment before and after chemotherapy

Domain /Test	CTx + (n=13)			CTx - (n=9)			<i>F</i>
	baseline	3 months f/u	<i>p</i>	baseline	3 months f/u	<i>p</i>	
Attention and concentration							
Digit Span Forward	10.8±3.0	10.2±3.2	0.407	9.2±2.3	9.9±1.9	0.322	0.863
Digit Span Backward	11.3±3.3	10.9±3.5	0.539	10.6±2.1	10.3±2.3	0.520	0.419
Digit span total	11.1±3.1	11.2±3.0	0.711	9.6±2.1	9.9±1.9	0.576	0.491
Spatial span forward	36.0±33.8	41.6±33.0	0.362	27.1±32.7	22.6±25.6	0.474	0.155
Spatial span backward	79.5±14.5	72.4±20.3	0.260	69.1±26.6	71.3±28.6	0.776	0.020*
Memory							
Rey-Kim memory quotient,	102.5± 14.1	108.2± 10.3	0.131	108.7±12. 0	110.6±11. 7	0.326	0.072
AVLT sum	10.4±3.0	11.6±1.8	0.047*	12.1±3.6	11.5±2.6	0.310	0.632
AVLT delayed recall	9.5±2.6	10.2±2.1	0.248	11.0±2.2	11.9±2.0	0.159	0.069
AVLT delayed recognition	9.6±3.7	10.4±3.5	0.117	11.0±2.7	12.8±2.5	0.068	0.011*
KCFT copy (ageSS)	14.7±1.8	14.3±2.1	0.910	14.3±5.1	14.6±2.0	0.563	0.927
KCFT immediate recall (ageSS)	13.1±3.7	14.2±2.0	>0.999	14.3±1.9	14.3±1.8	0.145	0.305

KCFT							
delayed recall (ageSS)	12.9±3.6	14.5±1.9	0.674	13.7±2.3	14.0±2.0	0.116	0.150
Executive Function							
STROOP (%)	56.0±41.1	48.2±37.6	0.097	56.2±37.3	60.4±34.2	0.631	<0.001*

CTx+: Patients Treated with Chemotherapy; CTx-: Patients Not Treated with Chemotherapy; AVLT: Auditory Verbal Learning Test; KCFT: Korean complex figure test; ageSS: age corrected scaled scores; f/u: follow-up

2. Neurocognitive results

We compared the neurocognitive results of the CTx+ group and the CTx- group (Table 3). Repeated-measures ANOVA demonstrated significant between-group differences over time in the spatial span backward test ($p=0.020$), the auditory verbal learning test (delayed recognition, $p=0.001$) and the stroop test ($p<0.001$).

3. Neuroimaging analysis

A. voxel based morphometry analysis

Comparing the CTx+ group and the CTx- group, there was neither significant group difference nor group-by-time interaction.

B. Diffusion tensor imaging analysis

Compared to CTx- group, CTx+ group patients showed decreased FA and increased MD in left hippocampus (Figure 3).

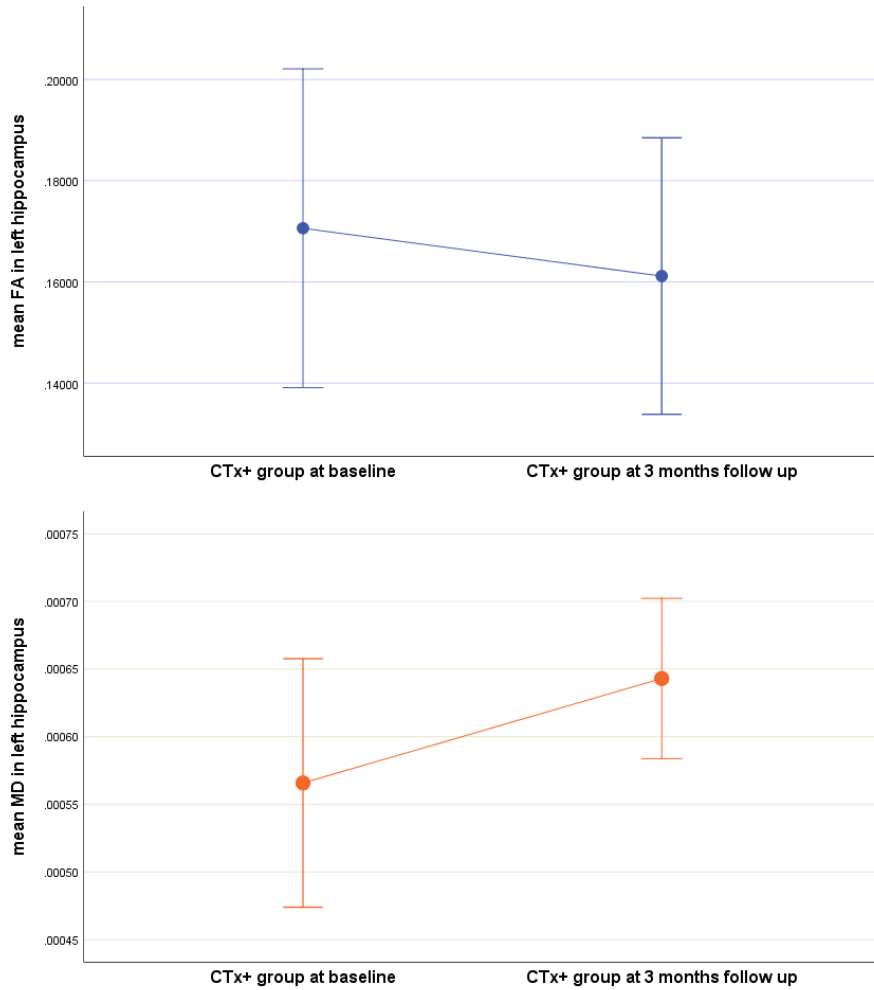


Figure 2. Decreased mean FA and increased mean MD among CTx+ group at 3 months follow up as compared to CTx+ group at baseline in left hippocampus. (Notes: CTx+: Patients Treated with Chemotherapy; CTx-: Patients Not Treated with Chemotherapy; FA: fractional anisotropy; MD: mean diffusivity)

C. Resting state functional connectivity analysis

(1) Region of interest (ROI) – based functional connectivity analysis

When seeding from the right and left hippocampus, there was no significant group difference of the functional connectivity between the CTx+ group and the CTx- group. However, functional connectivity analysis showed significant group-by-time interaction in the anterior thalamus (Table 4, Figure 2). Post-hoc analysis using ROIs of the hippocampus subfields showed significant group-by-time interaction of the left CA – anterior thalamus functional connectivity, the left subiculum – precuneus functional connectivity, and the right subiculum – paracentral gyrus functional connectivity (Table 5).

In all region of interest-based functional connectivity analysis result except hippocampus based analysis, there was no significant difference from between group analysis, within group analysis, and group-by-time interaction analysis.

Table 4. Brain regions showing significant group by time interaction in the hippocampus-based functional connectivity analysis.

Region	side	BA	K	T _{max}	Coordinates		
					x	y	z
Functional connectivity with left hippocampus							
Thalamus, anterior nuclei	Left		305	5.29	-8	-6	-8
				4.82	-4	-12	12
	Right		3.86	6	-10	12	

Table 5. Brain regions showing significant group by time interaction in the 6 hippocampal subfields-based functional connectivity analysis.

Region	side	BA	K	T _{max}	Coordinates		
					x	y	z
Functional connectivity with left cornu ammonis							
Thalamus, anterior nuclei	Right		228	4.92	2	-10	14
Functional connectivity with left subiculum							
Precuneus	Left	7	122	5.14	-6	-58	56
Functional connectivity with right subiculum							
Paracentral gyrus	Left	4	122	4.49	-12	-20	66
				4.17	-10	-24	58

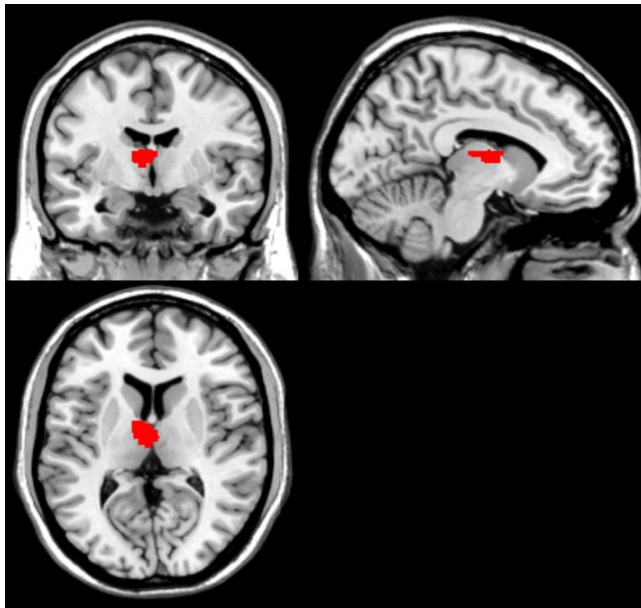


Figure 3. When seeding from the left hippocampus, functional connectivity analysis showed significant group-by-time interaction in the anterior thalamus (red).

(2) Graph-based network analysis: Minimum spanning tree analysis

When comparing minimum spanning tree outcomes (diameter, kappa, leaf and tree hierarchy for CTx+ group, CTx- group and HC group), between group comparison showed no statistically significant difference and longitudinal within group comparison showed no statically significant difference as well. In addition, We performed permutation analyses to test for possible alterations of the nodal characteristics degree and betweenness centrality. However no statistically significant difference was found in both between group and longitudinal within group comparisons regarding CTx+ group, CTx- group and HC group.

IV. DISCUSSION

To our knowledge, this study is the first multimodal longitudinal magnetic resonance imaging study on chemotherapy-induced cognitive impairment in gastric cancer patients. In this prospective and longitudinal study, we identified that compared to CTx- group, CTx+ group resulted in dysfunction in attention, memory, executive function in short term follow up 3 months after chemotherapy. Result of diffusion tensor image analysis demonstrated change in white matter integrity in left hippocampus. Resting state fMRI analysis with hippocampus, key region of cognitive function, set as seed, identified alteration of left hippocampus – anterior thalamus connectivity in chemobrain. Moreover, additional analysis of subfields of hippocampus identified alteration of left CA – anterior thalamus connectivity. Through these findings, we were able to confirm evidence of neuropathological change in chemobrain and qualitatively different neural changes in CTx+ group compared to CTx- group. However, voxel based morphometry analysis conducted to find brain structural change and minimum spanning tree analysis conducted to find brain network organization change resulted in no change.

Considering the divergence of opinion surrounding existence of chemobrain and questions such as “Is chemobrain a phenomenon that really exist?” in place, our finding has significant clinical meaning. Interestingly, results from structural analysis in our study shows no difference in hippocampal volume, but intrinsic hippocampal functional connectivity change and hippocampal microstructural abnormalities were identified in chemobrain. In existing cross-sectional researches on hippocampal volume change in chemobrain showed inconsistent finding according to time interval after chemotherapy with some reporting reduced total volume^{21,22,67}, and others reporting no change⁶⁸. Considering that changes in white matter and functional connectivity precede structural change in brain, it can be assumed that the reason behind no change in hippocampal volume in chemobrain is because short-term acute impact was evaluated.

Furthermore, as widely known, hippocampus is a key domain in cognitive function and a domain that is involved in pathogenesis of neurodegenerative disorder^{69,70}. This finding that detected change in hippocampus is in line with recent researches of prodromal Alzheimer's dementia; it can be interpreted that compared volumetric analysis methods, diffusion tensor image measures of the hippocampus results reflect more sensitive cognitive impairment in early stage^{71,72}. In mild cognitive impairment, which is clinical surrogate marker of incipient Alzheimer's dementia, while findings regarding change in gray matter volume are still ambiguous and inconsistent⁷³, at the beginning stage of cognitive dysfunction such as mild cognitive impairment, diffusion tensor image measures is being revealed as a very useful tool for detecting subtle ultrastructural brain tissue alteration before brain atrophy or neuronal degradation is identified as macroscopic level⁷⁴. Previous studies have shown that hippocampal MD is a better predictor in predicting progress from mild cognitive impairment to dementia than volume measures. The fact that findings shown in early stage of neurodegenerative disease was found in this research results suggests neurotoxicity of chemotherapy. Moreover, this suggest that we should more closely evaluate and continuously follow up with patients who underwent chemobrain symptoms for therapeutic intervention.

In particular, in this study, we were able to identify changes in diffusion tensor image measures in left hippocampus. Hippocampal asymmetry in patients with Alzheimer's dementia has often been identified in earlier studies^{75,76}. In addition, past studies have suggested that left hippocampus is more intimately involved in earlier stage of the process of neurodegenerative disorder than right hippocampus, and left hippocampus is potentially better neural biomarker for cognitive decline than right hippocampus⁷⁷. In the same vein, the results of this study show neural change that matches that of early stage of neurodegenerative disease, and more attention should be paid to changes in left hippocampus in the early stages of the chemobrain phenomenon.

Interestingly, through functional connectivity analysis, we were able to identify qualitatively different alteration of left hippocampus-anterior thalamus functional connectivity in CTx+ group compared to CTx- group. Anterior thalamus is a pivotal area in memory and cognition, and hippocampal-anterior thalamic interconnection is an area that plays vital role in human memory and cognition⁷⁸. In addition, the fact that change in the connectivity of hippocampal CA⁷⁹ and thalamus, which are known to be initially affected by neurodegenerative disorder such as Alzheimer's dementia, suggests that neural change due to chemobrain is similar to neural change due to early stage of neurodegenerative disorder. Therefore, in the future, study based on long term follow up of chemobrain should be carried out to study how resting state functional connectivity changes as chemobrain progresses.

Despite the clinical significance of chemotherapy-induced cognitive impairment, specific pathophysiological mechanism of chemotherapy-induced cognitive impairment has not been established well yet. Along with direct neurotoxic effects of chemotherapeutic agents, increased oxidative stress, immune dysregulation, blood-brain barrier disruption, etc. have been presented as potential pathophysiological mechanism of chemotherapy-induced cognitive impairment. Furthermore, as this hippocampus was highlighted through multimodal neuroimaging analysis in this study, studies identifying decreased neurogenesis and hippocampal cell proliferation in relation to chemotherapeutic agents are accumulating (Han et al., 2008a; Mustafa et al., 2008). In the future, there is a need for a comprehensive study to shed light on etiologies and pathogenesis of chemotherapy-induced cognitive impairment in order to accurately target the treatment that can make intervention for patients suffering from chemotherapy-induced cognitive impairment.

In this study, we have identified that adjuvant chemotherapy on gastric cancer patient adjuvant chemotherapy has an effect on dysfunction of attention, memory, executive function according to objective neurocognitive test. As it has

been known thus far, past studies show inconsistent result on cognitive impairment after chemotherapy due to reasons such as variability in study design and choice of comparison group ⁸⁰. Moreover, reviewing previous studies, we found that there are still many arguments regarding which domain's cognitive function chemobrain affects ⁸¹. This study has its strength because we enrolled subjects with normal cognitive functions in their 50s who had completed formal education in order to exclude factors such as age and cognitive reserve that can affect cognitive function. As such, based on our findings, cognitive impairment affects attention, memory, and executive function of gastric cancer patients after chemotherapy. Therefore, it is important that chemobrain symptoms after chemotherapy that are directly related to patient's quality of life should be evaluated and treated early.

There are several limitations in this study. This study was conducted with small sample size due to difficulty in gathering cancer patients as participants. This might be why we found no significant correlations between the neuroimaging analyses measures (functional connectivity strengths and DTI measures) and results of neurocognitive tests although we have identified changes in the regions of the brain that are associated with objective neurocognitive assessment nonetheless. Another limitation is that follow-up period was not long enough. Therefore, if further study is conducted with larger study population by longer follow-up can identify how cognitive impairment changes and furthermore how neural change appears, it should be more helpful to understand underlying mechanism of chemobrain. To our knowledge, this is the first longitudinal neuroimaging study on the effect of chemotherapy in gastric cancer patients. Our study shows adjuvant chemotherapy can cause decline in attention, memory and executive function of gastric cancer patients, accompanied by underlying neural change. Our study offers further evidence for the prevailing notion of cognitive alterations in patients after chemotherapy. Although basis underlying chemobrain is not clearly and universally explained, results from studies up to

now present hypothesis that pathological processes and clinical presentation of chemobrain is ultimately similar disease as age-related neurodegenerative disorder including mild cognitive impairment and Alzheimer's disease ⁸¹. Through looking also into studies on neurodegenerative disease including mild cognitive impairment and Alzheimer's disease, we confirmed hippocampal abnormalities in chemobrain. Result from this study helps in viewing underlying basis of chemobrain at a new angle and puts emphasis in importance of continuous assessment and intervention. In the future, longitudinal studies should be made with homogenous and larger sample of patients. These studies will deepen our understanding of underlying mechanism of chemobrain and will have significance by enabling more effective therapeutic intervention for patients.

V. CONCLUSION

This is the first longitudinal neuroimaging study on chemobrain in male gastric cancer patients. Following the findings from this study indicating that clinical presentation and neuropathological processes and centered on hippocampus of chemobrain is ultimately similar disease as age-related neurodegenerative disorder.

References

1. Berger AM, Shuster JL, Von Roenn JH. Principles and practice of palliative care and supportive oncology: Lippincott Williams & Wilkins; 2007.
2. Cull A, Hay C, Love S, Mackie M, Smets E, Stewart M. What do cancer patients mean when they complain of concentration and memory problems? *British journal of cancer* 1996;74:1674.
3. Ahles TA, Root JC, Ryan EL. Cancer-and cancer treatment-associated cognitive change: An update on the state of the science. *Journal of Clinical Oncology* 2012;30:3675.
4. Silberfarb PM. Chemotherapy and cognitive defects in cancer patients. *Annual Review of Medicine* 1983;34:35-46.
5. de Ruiter MB, Reneman L, Boogerd W, Veltman DJ, Van Dam FS, Nederveen AJ, et al. Cerebral hyporesponsiveness and cognitive impairment 10 years after chemotherapy for breast cancer. *Human brain mapping* 2011;32:1206-19.
6. Wefel JS, Schagen SB. Chemotherapy-related cognitive dysfunction. *Current neurology and neuroscience reports* 2012;12:267-75.
7. Koppelmans V, Vernooij MW, Boogerd W, Seynaeve C, Ikram MA, Breteler MM, et al. Prevalence of cerebral small-vessel disease in long-term breast cancer survivors exposed to both adjuvant radiotherapy and chemotherapy. *Journal of Clinical Oncology* 2015;33:588-93.
8. Simó M, Rifà-Ros X, Rodriguez-Fornells A, Bruna J. Chemobrain: a systematic review of structural and functional neuroimaging studies. *Neuroscience & Biobehavioral Reviews* 2013;37:1311-21.
9. Inagaki M, Yoshikawa E, Matsuoka Y, Sugawara Y, Nakano T, Akechi T, et al. Smaller regional volumes of brain gray and white matter demonstrated in breast cancer survivors exposed to adjuvant

- chemotherapy. *Cancer* 2007;109:146-56.
10. McDonald BC, Conroy SK, Ahles TA, West JD, Saykin AJ. Gray matter reduction associated with systemic chemotherapy for breast cancer: a prospective MRI study. *Breast cancer research and treatment* 2010;123:819-28.
 11. Deprez S, Amant F, Smeets A, Peeters R, Leemans A, Van Hecke W, et al. Longitudinal assessment of chemotherapy-induced structural changes in cerebral white matter and its correlation with impaired cognitive functioning. *Journal of Clinical Oncology* 2011;30:274-81.
 12. Deprez S, Amant F, Yigit R, Porke K, Verhoeven J, Stock JVD, et al. Chemotherapy-induced structural changes in cerebral white matter and its correlation with impaired cognitive functioning in breast cancer patients. *Human brain mapping* 2011;32:480-93.
 13. Kesler SR. Default mode network as a potential biomarker of chemotherapy-related brain injury. *Neurobiology of aging* 2014;35 Suppl 2:S11-S9.
 14. Feng Y, Tuluhong D, Shi Z, Zheng LJ, Chen T, Lu GM, et al. Postchemotherapy hippocampal functional connectivity patterns in patients with breast cancer: a longitudinal resting state functional MR imaging study. *Brain imaging and behavior* 2019:1-12.
 15. ELBeltagy M, Mustafa S, Umka J, Lyons L, Salman A, Tu C-YG, et al. Fluoxetine improves the memory deficits caused by the chemotherapy agent 5-fluorouracil. *Behavioural brain research* 2010;208:112-7.
 16. Lyons L, ELBeltagy M, Bennett G, Wigmore P. Fluoxetine counteracts the cognitive and cellular effects of 5-fluorouracil in the rat hippocampus by a mechanism of prevention rather than recovery. *PloS one* 2012;7.
 17. Acharya MM, Martirosian V, Chmielewski NN, Hanna N, Tran KK, Liao AC, et al. Stem cell transplantation reverses chemotherapy-induced cognitive dysfunction. *Cancer research* 2015;75:676-86.

18. Christie L-A, Acharya MM, Parihar VK, Nguyen A, Martirosian V, Limoli CL. Impaired cognitive function and hippocampal neurogenesis following cancer chemotherapy. *Clinical cancer research* 2012;18:1954-65.
19. Oz M, Atalik KEN, Yerlikaya FH, Demir EA. Curcumin alleviates cisplatin-induced learning and memory impairments. *Neurobiology of learning and memory* 2015;123:43-9.
20. Ramalingayya GV, Cheruku SP, Nayak PG, Kishore A, Shenoy R, Rao CM, et al. Rutin protects against neuronal damage in vitro and ameliorates doxorubicin-induced memory deficits in vivo in Wistar rats. *Drug design, development and therapy* 2017;11:1011.
21. Apple AC, Ryals AJ, Alpert KI, Wagner LI, Shih P-A, Dokucu M, et al. Subtle hippocampal deformities in breast cancer survivors with reduced episodic memory and self-reported cognitive concerns. *NeuroImage: Clinical* 2017;14:685-91.
22. Cheng H, Li W, Gong L, Xuan H, Huang Z, Zhao H, et al. Altered resting-state hippocampal functional networks associated with chemotherapy-induced prospective memory impairment in breast cancer survivors. *Scientific reports* 2017;7:45135.
23. Squire LR, Ojemann JG, Miezin FM, Petersen SE, Videen TO, Raichle ME. Activation of the hippocampus in normal humans: a functional anatomical study of memory. *Proceedings of the National Academy of Sciences* 1992;89:1837-41.
24. Richard GR, Titiz A, Tyler A, Holmes GL, Scott RC, Lenck-Santini PP. Speed modulation of hippocampal theta frequency correlates with spatial memory performance. *Hippocampus* 2013;23:1269-79.
25. Gordon BA, Shelton JT, Bugg JM, McDaniel MA, Head D. Structural correlates of prospective memory. *Neuropsychologia* 2011;49:3795-800.
26. Mueller SG, Schuff N, Yaffe K, Madison C, Miller B, Weiner MW.

- Hippocampal atrophy patterns in mild cognitive impairment and Alzheimer's disease. *Human brain mapping* 2010;31:1339-47.
27. Jung K-W, Won Y-J, Kong H-J, Lee ES. Cancer statistics in Korea: incidence, mortality, survival, and prevalence in 2016. *Cancer research and treatment: official journal of Korean Cancer Association* 2019;51:417.
 28. Oh C-M, Won Y-J, Jung K-W, Kong H-J, Cho H, Lee J-K, et al. Cancer statistics in Korea: incidence, mortality, survival, and prevalence in 2013. *Cancer research and treatment: official journal of Korean Cancer Association* 2016;48:436.
 29. Ahles TA, Root JC, Ryan EL. Cancer- and Cancer Treatment–Associated Cognitive Change: An Update on the State of the Science. *Journal of Clinical Oncology* 2012;30:3675-86.
 30. Etemadi A, Safiri S, Sepanlou SG, Ikuta K, Bisignano C, Shakeri R, et al. The global, regional, and national burden of stomach cancer in 195 countries, 1990–2017: a systematic analysis for the Global Burden of Disease study 2017. *The Lancet Gastroenterology & Hepatology* 2020;5:42-54.
 31. Dhobi MA, Wani KA, Parray FQ, Wani RA, Wani ML, Peer G, et al. Gastric cancer in young patients. *International journal of surgical oncology* 2013;2013.
 32. Ahles TA, Saykin AJ, McDonald BC, Furstenberg CT, Cole BF, Hanscom BS, et al. Cognitive function in breast cancer patients prior to adjuvant treatment. *Breast cancer research and treatment* 2008;110:143-52.
 33. Hermelink K, Untch M, Lux MP, Kreienberg R, Beck T, Bauerfeind I, et al. Cognitive function during neoadjuvant chemotherapy for breast cancer: results of a prospective, multicenter, longitudinal study. *Cancer* 2007;109:1905-13.

34. Nayak L, Lee EQ, Wen PY. Epidemiology of brain metastases. *Current oncology reports* 2012;14:48-54.
35. Go PH, Klaassen Z, Meadows MC, Chamberlain RS. Gastrointestinal cancer and brain metastasis. *Cancer* 2011;117:3630-40.
36. Broadbent DE, Cooper PF, FitzGerald P, Parkes KR. The cognitive failures questionnaire (CFQ) and its correlates. *British journal of clinical psychology* 1982;21:1-16.
37. Beck AT, Steer RA, Brown GK. Beck depression inventory-II. San Antonio 1996;78:490-8.
38. Steer RA, Beck AT. Beck Anxiety Inventory. 1997.
39. First MB, Spitzer RL, Gibbon M, Williams JB. Structured clinical interview for DSM-IV axis I disorders. New York: New York State Psychiatric Institute 1995.
40. Ashburner J. A fast diffeomorphic image registration algorithm. *Neuroimage* 2007;38:95-113.
41. Leemans A, Jeurissen B, Sijbers J, Jones D. ExploreDTI: a graphical toolbox for processing, analyzing, and visualizing diffusion MR data. *Proc Intl Soc Mag Reson Med*; 2009. p.3537.
42. Leemans A, Jones DK. The B-matrix must be rotated when correcting for subject motion in DTI data. *Magnetic Resonance in Medicine: An Official Journal of the International Society for Magnetic Resonance in Medicine* 2009;61:1336-49.
43. Tax CM, Otte WM, Viergever MA, Dijkhuizen RM, Leemans A. REKINDLE: robust extraction of kurtosis INDices with linear estimation. *Magnetic Resonance in Medicine* 2015;73:794-808.
44. Veraart J, Sijbers J, Sunaert S, Leemans A, Jeurissen B. Weighted linear least squares estimation of diffusion MRI parameters: strengths, limitations, and pitfalls. *Neuroimage* 2013;81:335-46.
45. Rohlfing T, Zahr NM, Sullivan EV, Pfefferbaum A. The SRI24

- multichannel atlas of normal adult human brain structure. *Human brain mapping* 2010;31:798-819.
46. Klein S, Staring M, Murphy K, Viergever MA, Pluim JP. Elastix: a toolbox for intensity-based medical image registration. *IEEE transactions on medical imaging* 2009;29:196-205.
 47. Eickhoff SB, Stephan KE, Mohlberg H, Grefkes C, Fink GR, Amunts K, et al. A new SPM toolbox for combining probabilistic cytoarchitectonic maps and functional imaging data. *Neuroimage* 2005;25:1325-35.
 48. Whitfield-Gabrieli S, Nieto-Castanon A. Conn: a functional connectivity toolbox for correlated and anticorrelated brain networks. *Brain connectivity* 2012;2:125-41.
 49. Woolrich MW, Jbabdi S, Patenaude B, Chappell M, Makni S, Behrens T, et al. Bayesian analysis of neuroimaging data in FSL. *Neuroimage* 2009;45:S173-S86.
 50. Smith SM. Fast robust automated brain extraction. *Human brain mapping* 2002;17:143-55.
 51. Jenkinson M, Bannister P, Brady M, Smith S. Improved optimization for the robust and accurate linear registration and motion correction of brain images. *Neuroimage* 2002;17:825-41.
 52. Jenkinson M, Smith S. A global optimisation method for robust affine registration of brain images. *Medical image analysis* 2001;5:143-56.
 53. Power JD, Barnes KA, Snyder AZ, Schlaggar BL, Petersen SE. Spurious but systematic correlations in functional connectivity MRI networks arise from subject motion. *Neuroimage* 2012;59:2142-54.
 54. Satterthwaite TD, Elliott MA, Gerraty RT, Ruparel K, Loughhead J, Calkins ME, et al. An improved framework for confound regression and filtering for control of motion artifact in the preprocessing of resting-state functional connectivity data. *Neuroimage* 2013;64:240-56.
 55. Zhang Y, Brady M, Smith S. Segmentation of brain MR images through

- a hidden Markov random field model and the expectation-maximization algorithm. *IEEE transactions on medical imaging* 2001;20:45-57.
56. Power JD, Schlaggar BL, Petersen SE. Recent progress and outstanding issues in motion correction in resting state fMRI. *Neuroimage* 2015;105:536-51.
 57. Ciric R, Wolf DH, Power JD, Roalf DR, Baum GL, Ruparel K, et al. Benchmarking of participant-level confound regression strategies for the control of motion artifact in studies of functional connectivity. *Neuroimage* 2017;154:174-87.
 58. Pruim RH, Mennes M, Buitelaar JK, Beckmann CF. Evaluation of ICA-AROMA and alternative strategies for motion artifact removal in resting state fMRI. *Neuroimage* 2015;112:278-87.
 59. Pruim RH, Mennes M, van Rooij D, Llera A, Buitelaar JK, Beckmann CF. ICA-AROMA: A robust ICA-based strategy for removing motion artifacts from fMRI data. *Neuroimage* 2015;112:267-77.
 60. Power JD, Mitra A, Laumann TO, Snyder AZ, Schlaggar BL, Petersen SE. Methods to detect, characterize, and remove motion artifact in resting state fMRI. *Neuroimage* 2014;84:320-41.
 61. Yan C-G, Cheung B, Kelly C, Colcombe S, Craddock RC, Di Martino A, et al. A comprehensive assessment of regional variation in the impact of head micromovements on functional connectomics. *Neuroimage* 2013;76:183-201.
 62. Birn RM, Molloy EK, Patriat R, Parker T, Meier TB, Kirk GR, et al. The effect of scan length on the reliability of resting-state fMRI connectivity estimates. *Neuroimage* 2013;83:550-8.
 63. Tzourio-Mazoyer N, Landeau B, Papathanassiou D, Crivello F, Etard O, Delcroix N, et al. Automated anatomical labeling of activations in SPM using a macroscopic anatomical parcellation of the MNI MRI single-subject brain. *Neuroimage* 2002;15:273-89.

64. Stam C, Tewarie P, Van Dellen E, Van Straaten E, Hillebrand A, Van Mieghem P. The trees and the forest: characterization of complex brain networks with minimum spanning trees. *International Journal of Psychophysiology* 2014;92:129-38.
65. Tewarie P, van Dellen E, Hillebrand A, Stam CJ. The minimum spanning tree: an unbiased method for brain network analysis. *Neuroimage* 2015;104:177-88.
66. Kruskal JB. On the shortest spanning subtree of a graph and the traveling salesman problem. *Proceedings of the American Mathematical society* 1956;7:48-50.
67. Bergouignan L, Lefranc JP, Chupin M, Morel N, Spano JP, Fossati P. Breast cancer affects both the hippocampus volume and the episodic autobiographical memory retrieval. *PloS one* 2011;6.
68. Eichbaum MH, Schneeweiss A, Sohn C. Smaller regional volumes of gray and white matter demonstrated in breast cancer survivors exposed to adjuvant chemotherapy. *Cancer* 2007;110:224-5.
69. Buckner RL, Andrews-Hanna JR, Schacter DL. The brain's default network: anatomy, function, and relevance to disease. 2008.
70. Braak H, Braak E. Frequency of stages of Alzheimer-related lesions in different age categories. *Neurobiology of aging* 1997;18:351-7.
71. Müller MJ, Greverus D, Weibrich C, Dellani PR, Scheurich A, Stoeter P, et al. Diagnostic utility of hippocampal size and mean diffusivity in amnesic MCI. *Neurobiology of Aging* 2007;28:398-403.
72. Carlesimo GA, Cherubini A, Caltagirone C, Spalletta G. Hippocampal mean diffusivity and memory in healthy elderly individuals. A cross-sectional study 2010;74:194-200.
73. Van Petten C. Relationship between hippocampal volume and memory ability in healthy individuals across the lifespan: review and meta-analysis. *Neuropsychologia* 2004;42:1394-413.

74. Fellgiebel A, Wille P, Müller MJ, Winterer G, Scheurich A, Vucurevic G, et al. Ultrastructural Hippocampal and White Matter Alterations in Mild Cognitive Impairment: A Diffusion Tensor Imaging Study. *Dementia and Geriatric Cognitive Disorders* 2004;18:101-8.
75. Barnes J, Scahill RI, Schott JM, Frost C, Rossor MN, Fox NC. Does Alzheimer's disease affect hippocampal asymmetry? Evidence from a cross-sectional and longitudinal volumetric MRI study. *Dementia and geriatric cognitive disorders* 2005;19:338-44.
76. Geroldi C, Laakso MP, DeCarli C, Beltramello A, Bianchetti A, Soininen H, et al. Apolipoprotein E genotype and hippocampal asymmetry in Alzheimer's disease: a volumetric MRI study. *J Neurol Neurosurg Psychiatry* 2000;68:93-6.
77. Eckerström C, Olsson E, Borga M, Ekholm S, Ribbelin S, Rolstad S, et al. Small baseline volume of left hippocampus is associated with subsequent conversion of MCI into dementia: The Göteborg MCI study. *Journal of the Neurological Sciences* 2008;272:48-59.
78. Aggleton JP, O'Mara SM, Vann SD, Wright NF, Tsanov M, Erichsen JT. Hippocampal–anterior thalamic pathways for memory: uncovering a network of direct and indirect actions. *European Journal of Neuroscience* 2010;31:2292-307.
79. Atienza M, Atalaia-Silva KC, Gonzalez-Escamilla G, Gil-Neciga E, Suarez-Gonzalez A, Cantero JL. Associative memory deficits in mild cognitive impairment: The role of hippocampal formation. *NeuroImage* 2011;57:1331-42.
80. Ahles TA, Root JC, Ryan EL. Cancer- and cancer treatment-associated cognitive change: an update on the state of the science. *Journal of clinical oncology : official journal of the American Society of Clinical Oncology* 2012;30:3675-86.
81. Ahles TA, Saykin AJ, McDonald BC, Li Y, Furstenberg CT, Hanscom

BS, et al. Longitudinal assessment of cognitive changes associated with adjuvant treatment for breast cancer: impact of age and cognitive reserve. *Journal of Clinical Oncology* 2010;28:4434.

ABSTRACT (IN KOREAN)

위암 환자에서의 항암화학요법 치료 이후 인지기능저하 현상에
대한 구조적, 기능적 뇌 영상 연구

<지도교수 정 영 철 >

연세대학교 대학원 의학과

안 재 은

위암 환자에서의 항암화학요법 이후 인지기능저하 현상의 임상적 중요성에도 불구하고, 아직까지는 항암화학요법 이후 인지기능저하 현상에 대한 종적 뇌영상 연구가 이루어진 바가 없다. 본 연구에서는 위암 환자에서의 항암 화학 요법 이후 인지 기능 저하 현상 기저의 뇌의 구조적, 기능적 변화를 탐색하기 위해 13명의 항암 화학 요법을 시행 받은 위암 환자, 9명의 항암 화학 요법을 시행 받지 않은 위암 환자, 10명의 정상 대조군을 모집하였다. 연구에 참여한 항암 화학 요법을 시행 받은 위암 환자 피험자들은 수술 후 항암화학요법 시행 전과 항암화학요법 시행 3개월 후 두 차례에 걸쳐 자가보고식 설문지, 신경인지검사, 뇌영상 검사를 시행하였다. 항암 화학 요법을 시행 받지 않은 위암 환자와 정상 대조군 또한 동일한 기간을 두고 기저점과 추적 관찰 시점에 동일한 검사들을 시행하였다. 연구 결과 항암 화학 요법 치료를 받지 않은 위암 환자 군에 비해, 항암 화학 요법 치료를 받은 위암 환자 군에서 주의력, 실행 기능 및 지연된 재인 기능이 유의미하게 저하되는

소견이 관찰 되었다. 더하여 항암 화학 요법 치료를 받은 위암 환자 군에서 항암 화학 요법 치료를 받지 않은 위암 환자 군에 비해 확산 텐서 영상 분석 연구 결과 좌측 해마에서 분획 이방성(fractional anisotropy)이 유의미하게 감소하고, 평균 확산성(mean diffusivity)이 유의미하게 증가하는 소견이 확인되었다. 더하여 휴지기 기능성 뇌 자기공명영상 연구 결과 좌측 해마와 전측 시상에서의 통계적으로 유의미한 수준의 그룹간 시간(group-by-time interaction)에 따른 상호작용이 관찰되었다. 하지만, 화소 기반 형태 분석(Voxel based morphometry) 결과에서는 의미 있는 뇌의 구조적 변화가 관찰되지 않았다. 본 연구는, 위암 환자에서 발생하는 항암 화학 요법 이후 인지 기능 저하 현상에 대한 최초의 종적 뇌영상 연구이다. 본 연구 결과는 항암 화학 요법 이후 인지 기능 저하 현상이 노화와 연관된 신경 퇴행성 질환(neurodegenerative disorder)과 유사한 임상적 변화와 신경 병리학적(neuropathological) 변화를 보임을 시사한다.

핵심되는 말: 위암, 항암 화학 요법 후 인지 기능 저하, 뇌영상 연구, 화소 기반 형태분석법, 확산 텐서 영상, 기능적 뇌자기공명영상